Catalysis Communications 25 (2012) 32–35

Contents lists available at SciVerse ScienceDirect

Catalysis Communications

journal homepage: www.elsevier.com/locate/catcom

Short Communication

Electrospun nanofibers of $ZnO/BaTiO_3$ heterostructures with enhanced photocatalytic activity

Pengrong Ren, Huiqing Fan *, Xin Wang

State Key Laboratory of Solidification Processing, School of Materials Science and Engineering, Northwestern Polytechnical University, Xi'an 710072, China

ARTICLE INFO

Article history:
Received 3 February 2012
Received in revised form 25 March 2012
Accepted 4 April 2012
Available online 9 April 2012

Keywords:
$BaTiO_3$
ZnO
Heterostructures
Photocatalytic

ABSTRACT

$ZnO/BaTiO_3$ nanofiber heterostructures with highly uniformly dispersed ZnO nanoparticles grown on primary $BaTiO_3$ nanofibers have been obtained by the combination of an electrospinning and a hydrothermal process. Powder X-ray diffraction (XRD), scanning electron microscopy (SEM) and transmission electron microscopy (TEM) were used to characterize the $ZnO/BaTiO_3$ nanofiber heterostructures. Furthermore, their UV-induced catalytic activities were studied by a degradation reaction of methyl orange (MO) dye. Compared with pure ZnO powders, $ZnO/BaTiO_3$ nanofiber heterostructures showed better performance of the photocatalytic property, which was ascribed to the synergistic effects of photogenerated electron and hole pair separation and high specific surface area.

1. Introduction

In the last decades, photocatalysis, as a "green" technique, has aroused great attention for its efficiency and broad applicability to eliminate toxic chemicals in the environment [1]. It has been reported that many nanostructural semiconductor metal oxides can degrade various organic pollutants under UV or visible light irradiation [2–6]. Currently the key focus to improve efficiency of photocatalysis is to inhibit the quick recombination of photoinduced charge carriers. Thus, semiconductor materials with heterostructures are applied because of the effective electron hole pair separation [7–9].

Among various heterostructures, nanofiber heterostructures are thought to be one of the most promising solutions. On the one hand, nanofibers, mainly prepared by electrospinning technology, have been proven to be effective supports owing to their high porosity and large surface area. The high porosity of a nonwoven mat of nanofibers usually enables direct growth of secondary nanostructures via heterogeneous nucleation [10]. The successful employment of electrospun nanofibers as substrates for other metal oxide nanostructures has been demonstrated for a number of reactions [11–13].

On the other hand, the separation of the nanostructural photocatalysts from the solution after a reaction is another challenge in a practical photocatalytic process. In order to solve this problem, using nanofibers as catalysts is a good choice since they can be easily separated from the solution due to the large length-to-diameter ratio. Additionally, the as-electrospun nanofibers could be reclaimed by sedimentation without a decrease in photocatalytic activity [14].

Zinc oxide (ZnO) nanomaterials, naturally n-type semiconductors with a wide band gap (Eg = 3.37 eV), have been recognized as an excellent material for photocatalytic processes [15]. Besides, barium titanate ($BaTiO_3$), a well-known perovskite-type multi metallic oxide with a band gap of 3.14 eV, has a great potential for optoelectronics [16]. More interestingly, $BaTiO_3$ offers favorable energy for photocatalysis since its conduction band edge is lower than ZnO [17]. In this regard, under UV light irradiation, a proper combination of $BaTiO_3$ and ZnO can lead to not only the transfer of electron from the conduction band of ZnO to that of $BaTiO_3$, but also the transfer of hole from the valence band of $BaTiO_3$ to that of ZnO. As such, the improved separation between photogenerated electrons and holes is expected to improve the photocatalytic activity of ZnO. A similar effect was also found in the $SrTiO_3/TiO_2$ nanofiber heterostructures [18].

On the basis of the above discussion, ZnO nanoparticles and $BaTiO_3$ nanofibers were chosen as the candidates for the heterojunction system. $ZnO/BaTiO_3$ heterostructures were obtained by the combination of an electrospinning and a hydrothermal process.

2. Experimental

2.1. Preparation of $ZnO/BaTiO_3$ nanofiber heterostructures

The experimental process included two steps. In the first step, 1 mL of tetrabutyl titanate and 0.747 g of barium acetate were dissolved in 1.5 mL of acetic acid and 5 mL of ethanol. After stirring at room temperature for 2 h, the above homogeneous sol was added to 10 mL of polyvinylpyrrolidone (PVP) ethanolic solution (8 wt.%) with vigorous stirring

* Corresponding author. Tel.: +86 29 88494463; fax: +86 29 88492642.
E-mail address: hqfan3@163.com (H. Fan).

1566-7367/$ – see front matter
doi:10.1016/j.catcom.2012.04.003

at room temperature for 4 h. Then, the above precursor solutions were drawn into a hypodermic syringe for electrospinning. The positive voltage applied to the tip was 20 kV and the distance between the needle tip and the collector was 15 cm. Followed with calcinations in air at 600 °C for 2 h, $BaTiO_3$ electrospun nanofibers were obtained.

In the second step, ZnO nanoparticles were outgrown from the $BaTiO_3$ nanofibers by using a hydrothermal treatment reported by J. Li [19]. Zinc acetate and the obtained $BaTiO_3$ nanofibers (with the mass ratio of $ZnO:BaTiO_3 = 1:2$) were dissolved in ethanol and microwave-heated at 180 °C for 1 h. In comparison, pure ZnO powders were prepared with zinc acetate in the similar hydrothermal condition.

2.2. Characterization

Phase structure of the as-synthesized powders was examined by X-ray diffraction (XRD) with Cu-Kα radiation (λ = 1.5406 Å). The morphology was investigated using scanning electron microscopy (SEM) equipped with energy-dispersive X-ray spectroscopy (EDS) and transmission electron microscopy (TEM).

2.3. Photocatalytic activity measurements

The photocatalytic reaction suspension was prepared by adding the sample (20 mg) to 20 mL of MO solution with a concentration of 10 mg/L. The suspension was sonicated for 10 min and then stirred in the dark for 30 min to ensure an adsorption/desorption equilibrium. The suspension was then irradiated using UV light (50 W high-pressure mercury lamp with main emission wavelength 313 nm) under continuous stirring. Analytical samples were taken from the reaction suspension after various reaction times, and centrifuged at 6500 rpm for 5 min to remove the particles for spectral measurement.

3. Results and discussion

XRD patterns of the electrospun nanofibers are shown in Fig. 1. All diffraction peaks in Fig. 1(a) could be indexed as the tetragonal $BaTiO_3$ (JCPDS No. 05-0626). After the hydrothermal reaction at 180 °C for 1 h, as shown in Fig. 1(b), additional diffraction peaks with 2θ values of 34.51°, 36.34°, 47.51°, 62.98°, 68.02° and 69.17° appeared, corresponding to (002), (101), (102), (103) (112) and (201) crystal planes of hexagonal ZnO, respectively (JCPDS No. 36-1451), indicating that ZnO was successfully formed in the hydrothermal reaction. Additionally, XRD peaks belonging to $BaTiO_3$ in the $ZnO/BaTiO_3$ heterostructures did not shift compared with pure $BaTiO_3$ nanofibers, which could be deduced that Zn did not substitute Ba or Ti and enter into the $BaTiO_3$ lattices.

Fig. 2(a) and (b) shows SEM images of the electrospun $BaTiO_3$ nanofibers and $ZnO/BaTiO_3$ nanofiber heterostructures, respectively. In Fig. 2(a), it could be seen that these randomly oriented $BaTiO_3$

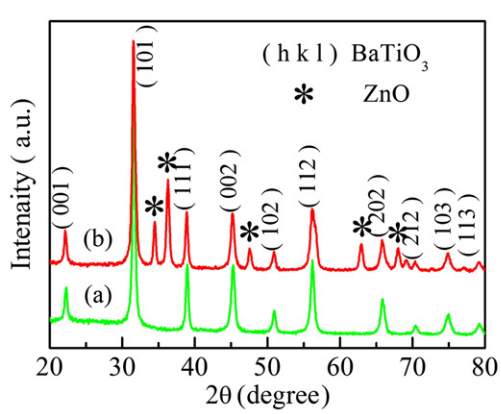

Fig. 1. XRD patterns of (a) $BaTiO_3$ nanofibers and (b) $ZnO/BaTiO_3$ nanofiber heterostructures.

nanofibers formed a network structure and had a relatively smooth surface. The length of $BaTiO_3$ nanofibers could reach several micrometers and the diameter of nanofibers was about 300–400 nm. After the hydrothermal reaction, as shown in Fig. 2(b), the $ZnO/BaTiO_3$ nanofiber heterostructures retained network structure and exhibited a rough surface due to the wrap of ZnO on the surface. Furthermore, Fig. 2(c) and (d) shows the EDS from the labeled region in Fig. 2(a) and (b), respectively. In Fig. 2(c), it is evident that the $BaTiO_3$ nanofibers were composed of Ba, Ti and O. The appearance of Al is due to the use of the aluminum foil in our SEM sample preparation. In Fig. 2(d), Al, Ba, Ti, and O were clearly detected.

Fig. 3(a) shows the typical TEM images of the electrospun $BaTiO_3$ nanofibers. It can be seen that the $BaTiO_3$ nanofibers were composed of nanoparticles and each nanoparticle was attached to several other nanoparticles. To further study the fine structures of the as-grown $BaTiO_3$ nanoparticles, the high-resolution transmission electron microscopy (HRTEM) was used. As shown in Fig. 3(b), well-developed lattice fringes were resolved and the lattice spacing measured from HRTEM was 4.04 Å, which agrees well with the distance between (001) plane of tetragonal $BaTiO_3$ phase. The low-magnification TEM image of the $ZnO/BaTiO_3$ nanofiber heterostructures is displayed in Fig. 3(c). It could be seen that the ultrasonic process during the sample preparation for TEM measurements did not cause the ZnO nanoparticles to fall off the $BaTiO_3$ nanofibers. It indicated that ZnO nanoparticles had been successfully grown onto the surface of the $BaTiO_3$ nanofibers. Meanwhile, the HRTEM image of $ZnO/BaTiO_3$ nanofiber heterostructures obtained from the area marked with circularity in Fig. 3(c) was shown in Fig. 3(d). The interplanar distances of 2.86 Å agree well with the lattice spacing of the (0002) planes of the hexagonal structured ZnO. Thus, the results confirmed that the successfully adopted synthesis route achieved $ZnO/BaTiO_3$ heterostructures, integrating ZnO nanoparticles and $BaTiO_3$ nanofibers.

Based on the SEM and TEM results, the possible two-step processes of $ZnO/BaTiO_3$ heterostructure formation are proposed. One process referred to the heterogeneous nucleation of ZnO on the $BaTiO_3$ nanofibers. For electrospun $BaTiO_3$ nanofibers, the high porosity and large surface area provided a lot of nucleation sites for the growth of ZnO nanostructures. The other process referred to the growth of ZnO nanoparticles. It is well-known that lattice mismatch plays an important role in the epitaxial growth of heterogeneous structures. A high degree of lattice mismatch prevents the nucleation and growth of an overlayer on a substrate because of the high structural strain. As a result, preferred growth of ZnO nucleus occurred at the interface with lower mismatch between ZnO and $BaTiO_3$ crystal plane. Finally, dispersed ZnO nanoparticles grew on the surface of $BaTiO_3$ nanofibers.

Furthermore, photocatalytic property of $ZnO/BaTiO_3$ nanofiber heterostructures was tested. Fig. 4 illustrates three times cycling MO degradation curves of C_t/C_0 versus time for photodegradation with pure ZnO powders and $ZnO/BaTiO_3$ nanofiber heterostructures as catalysts (C_0 is the original concentration of the MO and C_t is the real concentration at different times). Compared with the photodegradation result of ZnO powders, $ZnO/BaTiO_3$ nanofiber heterostructures had a much higher catalytic activity, which was also revealed in the ultraviolet–visible (UV–vis) spectra in the insets of Fig. 4. More importantly, it was indicated that these $ZnO/BaTiO_3$ nanofiber heterostructures with higher photocatalytic activity could be easily separated and recovered by sedimentation, as can be seen in Fig. 4 of three times cycling MO degradation curves.

A mechanism of improved photocatalytic activity of the $ZnO/BaTiO_3$ heterostructures is demonstrated in Fig. 5. It is known that photocatalytic processes are based on electron hole pairs generated by means of band gap excitation. The photoinduced electron and hole could migrate to the surface to react with the adsorbed reactants in the desired process, or undergo an undesired recombination. Therefore, the generation and separation of the photoinduced electron hole pairs are the key factors to influence a photocatalytic reaction. When the nanofibers of